# 行政院國家科學委員會專題研究計畫　成果報告

# (Ln1-xAxMn1-yBy03)系統物磁電特性研究及薄膜製作

計畫類別：個別型計畫
計畫編號：NSC91-2112-M-164-001-
執行期間：91 年 08 月 01 日至 92 年 07 月 31 日
執行單位：修平技術學院電機工程系

計畫主持人：陳宏仁

計畫參與人員：許進添　高銘政　王清吉　蕭聖芳

報告類型：精簡報告

處理方式：本計畫可公開查詢

中　華　民　國 92 年 10 月 30 日

# 行政院國家科學委員會專題研究成果報告

## (Ln1-xAxMn1-yByO3)系統物磁電特性研究及薄膜製作

計畫編號：NSC 91-2112-M-164-001-
執行期限：91 年 8 月 1 日至 92 年 7 月 31 日

主持人：陳宏仁副教授兼系主任　　修平技術學院電機工程系

## 一、中英文摘要

鈣鈦礦超巨磁阻材料 $La_{0.7}Pb_{0.3}Mn_{1-x}B_yO_3$ (B=Co and Fe)的結構、磁性及電性系統化的研究持續進行著。當 Mn 被 Co 及 Fe 部份取代時其結構扭曲不明顯主要是它們具相近的離子半徑。從 x-ray 結果知 Co 摻雜樣品具單相菱面體($R\bar{3}c$)結構，而 Fe 摻雜樣品結構從菱面體($R\bar{3}c$)轉變為斜方晶(Pbnm)。Co 及 Fe 摻雜量增加則鐵磁雙交換作用會逐漸被超交換作用取代。由 FC-ZFC 曲線顯示長程自旋序轉變為短程自旋序。所以 Mn 被 Co 及 Fe 取代會壓抑交換作用、降低鐵磁性及鐵磁轉變溫度。

Abstract

A systematic investigation of the structural, magnetic and electrical properties in the perovskite colossal magnetoresistance materials $La_{0.7}Pb_{0.3}Mn_{1-x}B_yO_3$ (B=Co and Fe) have been studied. The distortion induced by Mn-site substitution is not obvious due to the similar radius of Mn, Co and Fe. Powder x-ray diffraction patterns show a single phase of rhombohedral ($R\bar{3}c$) for Co doped system and a slight crystallographic transistion from rhombohedral ($R\bar{3}c$) to orthorhombic (Pbnm) symmetry for Fe doped system. Values of temperature dependence of magnetization indicate that the ferromagnetic double- exchange interaction is gradually substituted by the superexchange interaction. The ZFC-FC curves also indicate that long-range spin ordering is progressively substituted by the short-range spin ordering. The substi- tution of Mn by Co and Fe supresses the double-exchange interaction, decreases the ferromagnetism and the ferromagnetic transistion temperature.

## 二、緣由與目的

The mechanism of the CMR effect can be explained by double exchange model proposed by Zener[1]. The model introduces mobile $e_g$ electrons that mediate the ferromagnetic interaction between $Mn^{3+}$ and $Mn^{4+}$ via the intervening oxygen in the CMR manganites. The long-range ferromag- netic interaction can be perturbed when other ions are introduced into the manganese-site. The introduction may induce magnetic disorder and frustraction in these compounds that may lead to short-range spin order or eventually to a spin-glass stste. The results of several recent reaserches on the Ca, Sr contented compounds support the description [2, 3, 4]. Hence, to expolore the meachanism of CMR effect, it is important to investigate if the double-exhange and CMR effect could be obtained only directly by Mn. The elements Co and Fe exhibit similar radius and electronic configuration with Mn. Basing on this idea, we have performed reaserches on the structural and magnetic properties of the $La_{0:7}Pb_{0:3}(Mn_{1-x}Co_x)O_3$ and $La_{0:7}Pb_{0:3}(Mn_{1-x}$

$Fe_x)O_3$ compounds.

It is well known that the properties of hole-doped $La_{0.7}A_{0.3}MnO_3$ (A=Ca, Sr, Ba and Pb) depend on the exchange interaction between $Mn^{3+}$ ($t_{2g}^3e_g^1$) and $Mn^{4+}$($t_{2g}^3e_g^0$). Since the exchange energy is larger than the crystal field, the high-spin state is stable in Mn-content compounds [5]. Although lots of papers reported the properties of the small amounts of Fe substution on the Mn-site [6, 7] Figure 1 shows the electronic structure of $Mn^{3+}$ and $Fe^{3+}$. It is obvious the $e_g$ energy of Fe is lower than that of Mn. Thus there is only $Fe^{3+}$, $Mn^{3+}$ and $Mn^{4+}$ exist in these Fe-content $La_{0.7}Pb_{0.3}(Mn_{1-x}Fe_x)O_3$ compounds ($Mn^{4+}$ doesnot exist).

## 三、結果與討論

Polycrystalline bulk samples of the compounds $La_{0.7}Pb_{0.3}Mn_{1-x}B_yO_3$ (B=Co and Fe) were prepared by conventional ceramic fabrication technique of solid-state reaction. The powders were calcined twice in air at 850 ℃ for 24 hours with intermediate grindings, then pressed into disk-shaped pellets and finally sintered in air at 1175 ℃ for 72 hours. The structure and phase purity of the samples were examined by the powder *x*-ray diffraction using Cu-$K_\alpha$ radiation at room temperature. The magnetization measurements were performed by a Quantum Design MPMS superconducting quantum interference device (SQUID) magnetometer.

In the Co-content compounds, the trivalence Co ions are favor to be in low spin state $Co^{III+}$ ($t_{2g}^6e_g^0$) at low temperature, and progressively convert into high-spin state $Co^{3+}$ ($t_{2g}^4e_g^2$) as temperature increasing. The energy difference between these two spin state is so small as about 0.03 eV so that the thermal excitation can provide a conversion from low-spin state to highspin state [8, 9]. The tetravalence Co ions can be low-spin state $Co^{IV}$ ($t_{2g}^5e_g^0$) and high-spin state $Co^{4+}$ ($t_{2g}^3e_g^2$). A. Chainani et al: shows that the energy of high-spin state $Co^{4+}$ is about 1 eV lower than low-spin state $Co^{IV+}$ [10]. At this stage it will be interesting to study the effect of progressive substitution of Co for Mn in the $La_{0.7}Pb_{0.3}(Mn_{1-x}Co_x)O_3$.

The x-ray patterns of six representative samples with x=0.0, 0.2, 0.4, 0.6, 0.8, and 1.0 are shown in figure 2. Powder x-ray diffraction patterns shows single phase rhombohedral crystal structure with space group $R\bar{3}c$ for all samples. In this series of samples, the peaks of x-ray patterns gradually shift to higher degree from sample with x=0.0 to sample with x=1.0 due to smaller lattice parameters by gradually substituting cobalt in place of manganite. The decrease in the lattic parameters should be related to smaller ionic radii of Co ion. There are various ion radius of $Mn^{3+}$, $Mn^{4+}$, $Co^{3+}$, and $Co^{4+}$ in the $La_{0.7}Pb_{0.3}(Mn_{1-x}Co_x)O_3$ system. Where the ion radius of trivalent Co ion 0.55 $A^o$ in low-spin state; 0.61 $A^o$ in high state, and tetravalent Co is 0.53 $A^o$ in high-spin state. In addition, trivalent Mn ion radius is 0.58 $A^o$ in low-spin state; 0.65 $A^o$ in high-spin state, and tetravalent Mn is 0.53 $A^o$ in high-spin state.

The temperature dependence of magnetization taken from samples with $0.0 \le x \le 1.0$ are shown in figure 3. Magnetization (M) measurements were performed in magnetic field up to 5Tesla. The samples undergoes a paramagnetic (PM) to ferromagnetic (FM)

transition, consistent with the results reported previously. As Co is doped into the samples, both the FM transition temperate ($T_C$) and M are systematically lowered. Curie temperature of sample, x=0.0, 0.2, 0.4, 0.6 and 0.8 are 274 K, 223 K, 216 K, 198 K and 167 K, respectively. The Curie temperature $T_C$ is defined as the temperature where the dM/dT reaches the maximum value. A value of 67 emu/g with x=0.0 is deduced from the saturated value of the magnetizing curve at 5 K and 5 Tesla. The saturated value of magnetic moment decreased as Co doped increased.

The inverse susceptibility as a function of temperature are shown in figure 4. The reciprocal susceptibility indicates a characteristic of paramagnetic Curie-Weiss behavior. The paramagnetic susceptibility data can be usually approximated by $\chi=\chi_0+C/(T-T_C)$ where $\chi_0$ is a temperature independent component of the susceptibility, $C/(T-T_C)$ is the Curie-Weiss contribution. C is the Curie constant, and $T_C$ is the Curie temperature. A linear extrapolation of the high temperature paramagnetic $1/\chi$ values gives the paramagnetic Curie point qp indicating the existence of the short range order of spin clusters. Since Co doping is the direct replacement of $Mn^{3+}$ by $Co^{3+}$, the experimental result suggest that the sites occupied by $Co^{3+}$ can no longer effectively participate in the DE process. In these oxide samples, the 3d level of the Mn and Co ions are known to split into $t_{2g}\uparrow$, $e_g\uparrow$, $t_{2g}\downarrow$ and $e_g\downarrow$ due to the strong Hund's coupling. The con_gurations are $t_{2g}^3\uparrow e_g^2\uparrow$ for $Co^{3+}$, $t_{2g}^3\uparrow e_g^1\uparrow$ for $Co^{4+}$ and $Mn^{3+}$, and $t_{2g}^3\uparrow$ for $Mn^{4+}$, respectively. For these ions, the $t_{2g}\uparrow$ bands are fully occupied, the $t_{2g}\downarrow$ and $e_g\downarrow$ bands are empty, and the $e_g\uparrow$ depend on the election distribution of the Co and Mn ions. The ions of samples has shows that $Co^{3+}$, $Mn^{3+}$, and $Mn^{4+}$ are present, for lower x cases and $Co^{3+}$, $Co^{4+}$, and $Mn^{4+}$ are present for larger x cases. Therefore, it is suffient to consider only the high-spin $Co^{4+}$ which is strongly hybridized by the charge-transfer state. Other cobalts will remain in the trivalent low-spin state. The ferromagnetic DE interaction as x is close to 1 is considered to be predominantly present between such $Co^{3+}$ and $Co^{4+}$ spins. Since $Co^{3+}$ replaces $Mn^{3+}$, doping with Co causes a depletion of the $Mn^{3+}/Mn^{4+}$ ratio, the population of the hopping electrons, and the number of available hopping sites. Thus, DE is suppressed, resulting in the reduction of ferromagnetism and metallic conduction as Co dopping increasing. Therefore, the temperature dependence of the resistance at H = 0 tesla and at H = 5 teslas of $La_{0:7}Pb_{0:3}MnO_3$ without any Co doping measured as shown in figure 5. In zero field, the resistance exhibits a metallic behavior ($dR/dT>0$) at low temperature and a insulator behavior ($dR/dT<0$) at high temperature. A sharp resistance peak indicating a metal-insulator transition occurs around $T_P$ = 200K. When a magnetic field (H = 5 teslas) is applied, the temperature dependence of the resistance is similar to that in zero field, but the resistance decrease. The negative MR ratio value defined as $(R(H)-R(0))/R(0)$ is also plotted in figure 5 with a field of H = 5 teslas. MR value becomes as large as about 50% below 200 K and 25% around 300 K. Figure 6 shows the x-ray patterns of the six representative samples with x=0.0, 0.2, 0.4, 0.6, 0.8 and 1.0.

The powder x-ray diffraction spectra f sample x=0.0, 0.2 and 0.4 were indexed in rhombohedral crystal structure with space group $R\bar{3}c$ (No.167), while the other three compositions existed orthorhombic symmetrywith space group Pbnm (No.62). The peaks of x-ray patterns diminutively shift to higher degree in this series of samples due to the progressive substitution of Fe in the Mn-site. The consequence is owing to the reasons that the the average ionic radius of $Mn^{3+}/Mn^{4+}$ is smaller than $Fe^{3+}$. The radius of $Mn^{3+}$, $Mn^{4+}$ and $Fe^{3+}$ are 0.645 $A^o$, 0.53 $A^o$ and 0.645 $A^o$, respectively [12]. The similar ionic radii of $Fe^{3+}$ and $Mn^{3+}$ means that crystal distortion induced by Fe substitution may be ignored. However, it will be getting obvious of distortion as Fe substution increasing.

In order to survey the spin order and magnetic behavior, the zero-field-cool (ZFC) and field-cool (FC) magnetization curves were measured at a field of 100 Oe as shown in figure 7. DC Magnetization was measured in SQUID MPMSR2-5S system. In zero-field-cooled (ZFC) measurements the samples were cooled roomtemperature to 5 K in zero field. A field of 100 Oe was applied and then magnetization measurements were carried out as temperature increasing. For the cooled (FC) caes, the samples were cooled under an applied field of 100 Oe. The measurements were also carried out as that of ZFC case. The temperature dependence of reduced magnetization is shown in figure 8. For sample x=0.00, the magnetic moments increase sharply as the temperature decrease around the transition temperature. While the FC susceptibilities saturate below about $T_C$, the ZFC curves display a maximum and decrease slightly towards low temperatures. The near overlap of ZFC and FC curves composition clearly suggests a ferromagnetic long-range spin order. Conversely, the irreversibility between the ZFC and FC magnetization curves is clearly seen below ferromagnetic-paramagnetic (FMPM) transition temperature, $T_c$, for x=0.2 and 0.4 samples. The ZFC curves coincide with the FC curves at high temperature, but deviate from each other as the temperature is decreased. The ZFC-FC curves display the irreversibilityand λ-shape traces, suggesting the existence of a short-range spin order. The two end compounds exhibit distinct kinds of magnetic order. The $La_{0:7}Pb_{0:3}MnO_3$ has long-range spin order, while the light substution cases, $La_{0:7}Pb_{0:3}Mn_{0:8}Fe_{0:2}O_3$ and $La_{0:7}Pb_{0:3}Mn_{0:6}Fe_{0:4}O_3$, has short-range one. The reason for the variation is the introduction of Fe ions to the Mn-site can lead to a decreased occupation of ferromagnetic $Mn^{3+}$-$O^{2-}$-$Mn^{4+}$ bonds and, consequently, weaken the total DE interaction. As the substution value x is so large that most of the $Mn^{3+}$ be substutedby $Fe^{3+}$. The ferromagnetic $Mn^{3+}$-$O^{2-}$-$Mn^{4+}$ DE interaction would be replaced by antiferromagnetic $Fe^{3+}$-$O^{2-}$-$Mn^{4+}$ and $Fe^{3+}$-$O^{2-}$-$Fe^{3+}$ exchange coupling for x=0.6, 0.8 and 1.0.

The temperature dependence of magnetization taken from samples with $0.0 \leq x \leq 1.0$ are shown in figure 9. Magnetization (M) measurements were performed in magnetic field up to 5 T. The samples exhibit a paramagnetic (PM) to ferromagnetic (FM) transition for $x \leq 0.4$, consistent with the results stated in that of FC-ZFC results. As

Fe is doped into the samples, both the ferromagnetic transition temperate ($T_C$, defined as the temperature where the value of dM(T)/dT reaches the maximum value) and magnetization (M) are systematically lowered. Transition temperature of samples, x=0.0, 0.2 and 0.4 are 335 K, 179 K and 121 K, respectively. Values of 83.94 emu/g, 49.63 emu/g and 22.58 emu/g with x=0.0, 0.2and 0.4, respectively, are deduced from the saturated value of the magnetization curve at 5 K and 5 Tesla. The saturated value of magnetic moment decreased as Fe doped increased. For x large than 0.4, the paramagnetic-ferromagnetic transition vanish and antimagnetic phase appear due to the large amount of substution of $Mn^{3+}$ by $Fe^{3+}$.

## 四、計劃成果及自評

We have presented a systematical study of the magnetotransport behavior in the $La_{0.7}Pb_{0.3}Mn_{1-x}B_yO_3$ (B=Co and Fe) system. For the results of Mn-site substitution in the previous chapter, some concludsions are summarized as follows:

1. Powder x-ray diffraction patterns show a single phase of rhombohedral symmetry ($R\bar{3}c$) for Co doped system and a slight crystallographic transition from rhombo-hedral symmetry ($R\bar{3}c$) to orthorhombic (Pbnm) crystal structure for Fe doped system.
2. The saturation magnetization decreases obviously as Co or Fe doping content is increased. Values of temperature dependence of magnetization indicate that the ferro-magnetic double-exchange interaction is gradually substituted by the superexchange interaction.
3. The ZFC-FC curves also indicated that long-range spin ordering is progressively substituted by the short-range spin ordering. The substitution of Mn by Co and Fe supresses the double-exchange interaction, weakens the ferromagnetism and decreases the ferromagnetic transition temperature $T_C$.

The substitution of Co and Fe for Mn decrease the percentage of ferromagnetic $Mn^{3+}$-$O^{2-}$-$Mn^{4+}$. The role functions of all elements in these compounds had been clear up in this project. Based on the knowledge of these compounds, it would be helpful to control the physical mechanism and improve the characteristics on preparing their thin film devices in the future works.

## 五、參考文獻


1. C. Zener, Phys. Rev. **82,** 403 (1951).
2. A. Simopoulos et al:, Phys. Rev. B 59, 1263 (1999).
3. D. N. H. Nam et al:, Phys. Rev. B 59, 4189 (1999).
4. S. M. Yusuf et al:, Phys. Rev. B 62, 1118 (2000).
5. R. Mahendiran and A. K. Raychaudhuri, Phys. Rev. B 54, 11044 (1996).
6. L. Righi et al:, J. Appl. Phys. 81, 5767 (1997).
7. S. M. Yusuf et al:, Phys. Rev. B 62, 1118 (2000).
8. V. G. Bhide et al:, Phys. Rev. B 12, 2832 (1975).
9. M. A. Senaris-Rodriguez and J. B. Goodenough, J. Solid State Chem. 118, 323 (1995).
10. A. Chainani, M. Mathew and D. D. Sarma, Phys. Rev. B 46, 9976 (1992).
11. J. P. Zhou et al:, J. Appl. Phys. 75, 1146

(1999).
12. R. D. Shannon and C. T. Prewitt, Acta Crystallogr. Sec. A 32, 751 (1976).

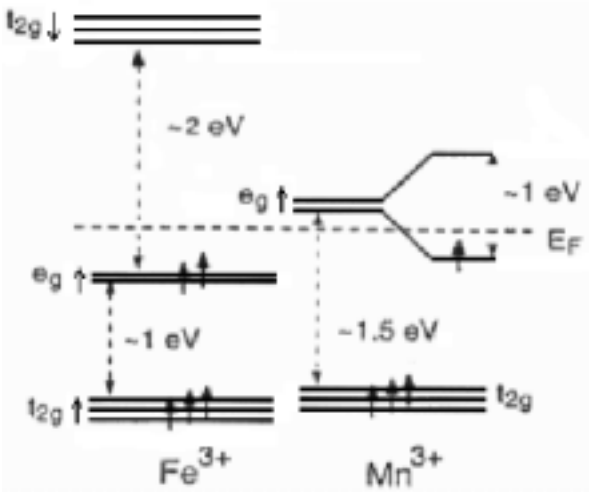


Fig. 1: Electronic structure of $Mn^{3+}$ and $Fe^{3+}$.

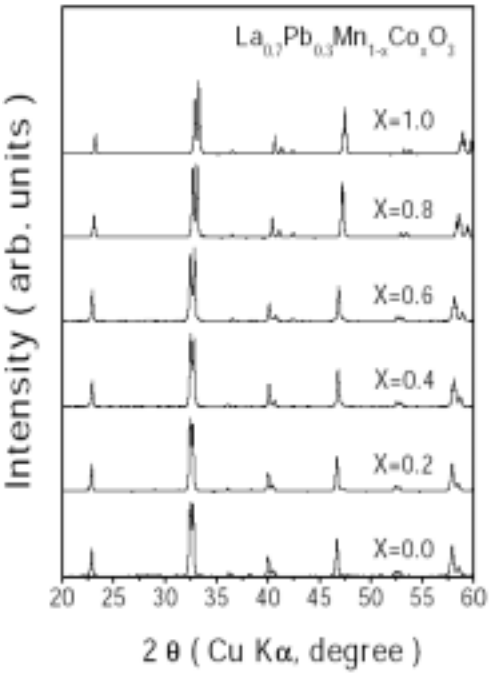


Fig. 2: x-ray diffraction patterns of the five representive samples with x=0.0, 0.2, 0.4, 0.6, 0.8, 1.0.

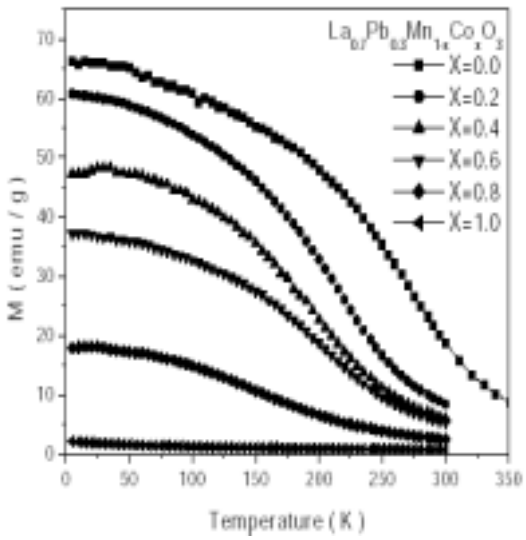


Fig. 3: Temperature dependence of magnetization been taken. Magnetization measurements were performed in magnetic field up to 5T.

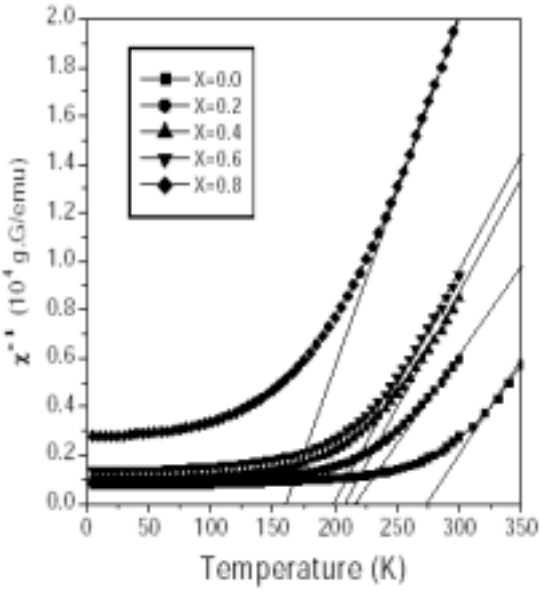


Fig. 4: Temperature dependence of inverse susceptibility taken from samples within $0.0 \leq x \leq 1.0$. The reciprocal susceptibility indicates a characteristic of paramagnetic Curie-Weiss behavior. The paramagnetic susceptibility data can be usually approximated by $\chi=\chi_0+C/(T-T_C)$.

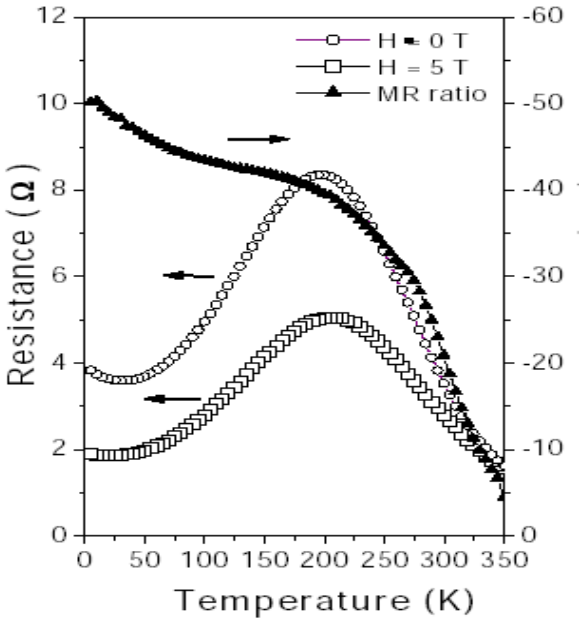


Fig. 5: The 5teslas as a function of temperature of $La_{0:7}Pb_{0:3}MnO_3$ without any Co doping.

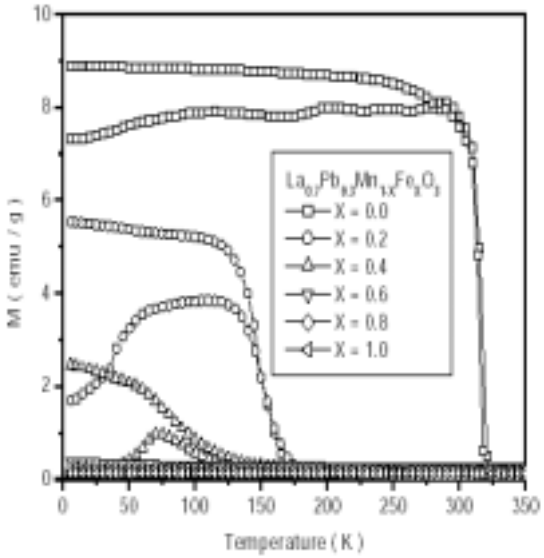


Fig. 7: ZFC and FC magnetization curves measured at a field of 100 Oe for all samples.

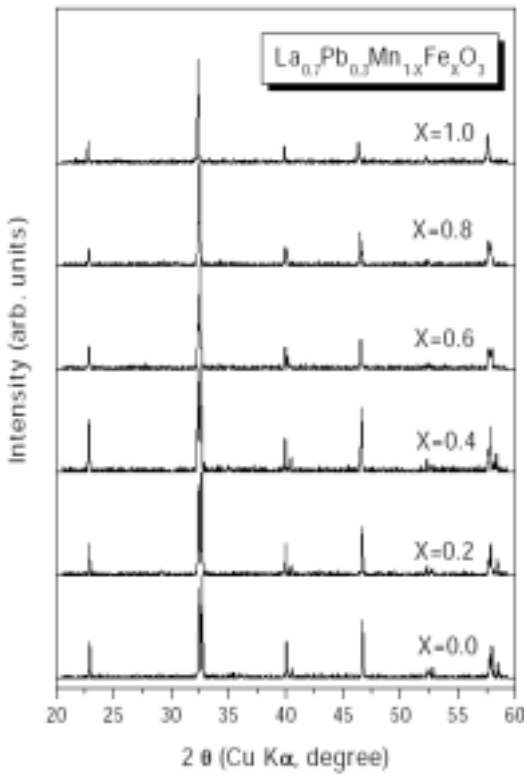


Fig. 6: x-ray diffraction patterns for all samples.

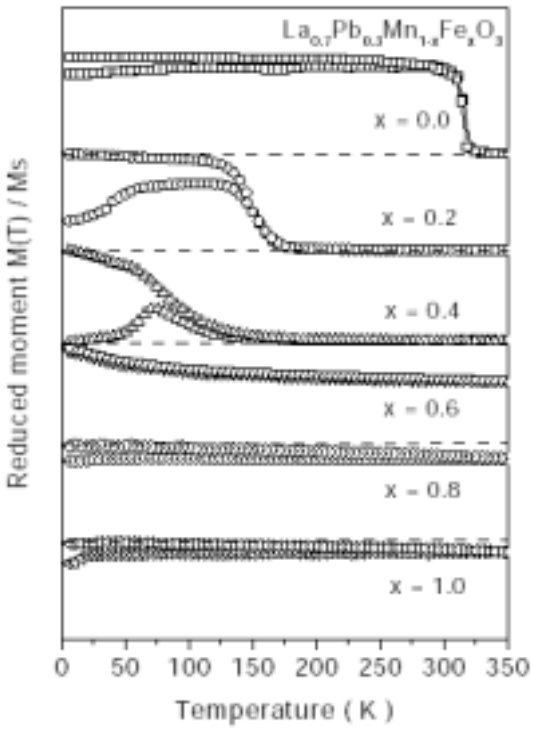


Fig. 8: ZFC and FC reduced magnetization curves measured at a field of 100 Oe for all samples.

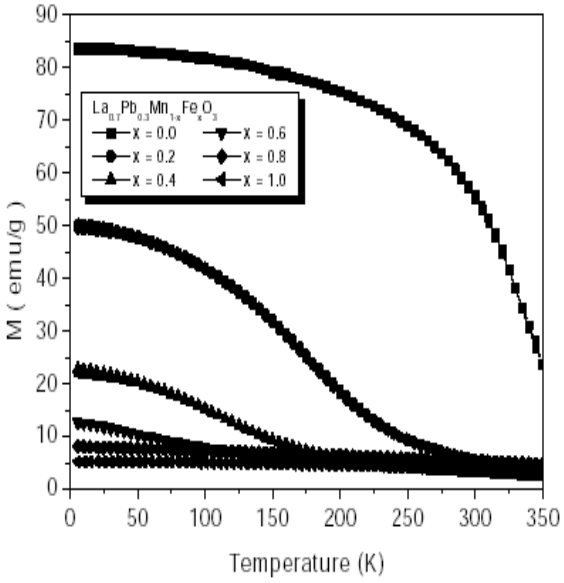


Fig. 9: Temperature dependence of magnetization measured at a field of 5 teslas for all samples.